IEEE Access
Multidisciplinary | Rapid Review | Open Access Journal

Received May 5, 2019, accepted May 31, 2019, date of publication June 10, 2019, date of current version June 25, 2019.

Digital Object Identifier 10.1109/ACCESS.2019.2921860

GNSS Measurements Model in Ship Handling Simulators

PAWEŁ ZALEWSKI AND MATEUSZ BILEWSKI
Faculty of Navigation, Maritime University of Szczecin, 70-500 Szczecin, Poland

Corresponding author: Paweł Zalewski (p.zalewski@am.szczecin.pl)

This work was supported by the Subsidy of the Polish Ministry of Science and Higher Education for Statutory Activities under Grant S/1/CIRM/2016.

ABSTRACT Electronic chart display and information system (ECDIS) forms the basis of contemporary and future marine e-navigation, track control, and integrated navigation systems, and is a key navigational aid in maritime ship handling simulators. All the ECDIS information is referred to as positioning, navigation, and timing (PNT) data derived from the global navigation satellite system (GNSS) by default. GNSS data fidelity, its representation, and accurate model of error propagation to ship final position are becoming the key factors enabling ship handling simulators to be utilized in navigators' training and research analyses of vessels' maneuvering. This paper presents an advanced stochastic model of GNSS code pseudorange observations and position-fix calculation based on GPS example. It has been developed for simulated GPS shipborne receivers interconnected to the ECDISs in physical and virtual reality ship simulators.

INDEX TERMS GNSS, GPS, ECDIS, simulation, ship handling, marine navigation.

I. INTRODUCTION

Simulation is used for a wide range of engineering, education, and research activities to replicate an existing system behavior under various conditions because it is faster or cheaper than performing tests in the ''physical – real world''. State-of-the-art hydrodynamic modeling allows virtual vessels, objects and physical equipment of modern ship bridge simulators to be utilized and interacted as in reality. Most of such ship handling simulators are certified to mariners training compliant with International Maritime Organization (IMO) Convention on Standards of Training, Certification and Watchkeeping for Seafarers (STCW) [4]. But the technical standards for STCW certification of ship handling simulators stipulate very general requirements for simulated Global Navigation Satellite System (GNSS) equipment. Specifically quoting after [4]: 1) GNSS interface should be realistic, 2) positioning reference systems should provide new position data with a refresh rate and accuracy suitable for the intended operations, 3) monitoring of positioning reference systems should include realistic alarms for any typical failure condition. There are no specific requirements, guidelines or recommendations on GNSS positioning error and its model. So, the realism of GNSS positioning in ship handling simulators is quite superficial while the fidelity of GNSS model becomes one of the critical issues of simulated environment's physical reality. Contemporary marine vessels are equipped with complex navigation and communication systems such as Electronic Chart Display & Information System (ECDIS), Automatic Identification System (AIS), Global Maritime Distress & Safety System (GMDSS), Integrated Navigation Systems (INS) which all rely on GNSS Positioning, Navigation and Timing (PNT) data [12]. The processing of these data can lead to functionalities long-established in aviation but still emerging in marine navigation, like positioning integrity assessment or interference, jamming, and spoofing mitigation (see [2], [5], [8], [9], [13], [18], [22], [23], [26], [27]). It is anticipated that such functionalities will be embedded in next generation autonomous surface ships. However they are becoming necessary even today onboard manned vessels as deliberate spoofing or intentional and incidental jamming is quite probable. Because of these identified threats and vulnerabilities of satellite navigation the proper and reliable modeling, processing, and presentation of PNT data in ship bridge simulators are essential for both research and training of seafarers. A state of the art GNSS telemetric model should be an indispensable item of any ship handling simulator that can simulate activities that deliberately affect accuracy of

The associate editor coordinating the review of this manuscript and approving it for publication was Halil Ersin Soken.

PNT data. A virtual receiver built upon such model can be equivalent to commercially available GNSS signal emulators [3], [10] but customized for a ship bridge simulator input/output and easier to operate by a ship handling instructor.

II. GNSS TELEMETRIC MODEL

The realistic simulation of GNSS measurement errors' propagation into the ship's WGS84 referenced position requires the implementation of a telemetry model that corresponds strictly to the one used in the real system. A GPS system is analyzed as an example equivalent to other GNSS subsystems (Glonass, Beidou, Galileo, Indian Regional Navigation System). A standard code-based point positioning GPS model should perform two main tasks: 1) compute the WGS84 Earth-centred, Earth-fixed (ECEF) positions ($X_S \in \mathbb{R}^3$) of satellites' antennas phase centers based on GPS ephemeris, 2) compute the WGS84 geodetic position ($X \in \mathbb{R}^3$) of the receiver's antenna phase center based on the visible satellites' (referred to as space vehicles' – SVs') ECEF positions and measured SVs' ranges. To achieve this goal, an algorithm corresponding to the one recommended in user interface specifications of GPS navigation [1], [6], [16] should be implemented in a ship bridge simulator. Research on maritime GNSS PNT and, especially, on the utilization of European Geostationary Navigation Overlay System (EGNOS) integrity data in the maritime domain [27], [28] has led into the development of an algorithm presented below and its implementation into the physical ship bridge simulator and the virtual reality ship bridge simulator (VRSS).

A. FROM GPS EPHEMERIDES TO ECEF SATELLITES' POSITIONS

Ephemerides of physical GPS SVs are broadcast to users as a part of the GPS signal in the navigation message. The ephemeris parameters enable calculation of SV ECEF position with an accuracy of about 5m (root mean squared error – RMS) at any observation epoch [19]. They are calculated by predicting orbits based on curve fitting 4 to 6 hours ahead of the most recent orbit data [25]. GPS SVs broadcast ephemeris and other technical parameters in a navigation message every 12.5 minutes, at the typical update rate of 2h. Many contemporary navigation and geodetic receivers can record these data in the Receiver Independent Exchange Format (RINEX) [11] and there are many International GNSS Service (IGS) and commercial GNSS reference stations which share RINEX data via the Internet. The data can be imported to a ship simulator's GPS subsystems either offline or online. Alternatively a reduced set of ephemeris parameters available online as almanac data can be sufficient for simulation scenarios not requiring accurate replication of GNSS measurements conditions and SVs positions. The real error of SV ECEF position calculated from almanac data reaches up to 2km (RMS) [19] but in a ship handling simulator this error can be modeled with much lower values.

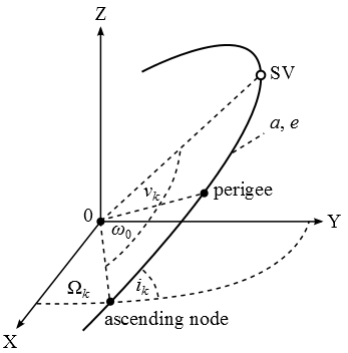

FIGURE 1. The orbital parameters of SV in ECEF frame.

RINEX navigation data files contain the following parameters of each SV marked by its unique pseudo-random noise code (PRN) number:

- t_{oc}: epoch (first data block): ephemerides broadcast date and time of the GPS clock [y m d h min s],
- l_s: number of leap seconds [s],
- a_0: SV clock bias [s],
- a_1: clock drift (the first derivative of the clock bias) [-],
- a_2: clock drift rate (the second derivative of the clock bias) [1/s],
- t_{oe}: ephemeris reference epoch of the current GPS week, the center of the interval over which the ephemeris is valid, presented in the unit of seconds [s],
- G_W: number of the GPS week to go with t_{oe} [-],
- orbital elements (the Keplerian parameters) at t_{oe}:
  - $\sqrt{a}$: square root of semi-major axis [$m^{1/2}$],
  - e: elliptical orbit eccentricity [-],
  - M_0: mean anomaly [rad],
  - Δ_n: variation of mean angular velocity [rad/s],
  - Ω_0: right ascension of the ascending node [rad],
  - i_0: the orbital inclination angle [rad],
  - ω_0: argument of periapsis (the angle from the body's ascending node to its periapsis) [rad],
- $\dot{\Omega}$: right ascension of the ascending node change rate [rad/s],
- i': orbital inclination change rate [rad/s],
- $C_{\omega c}$,$C_{\omega s}$,C_{rc},C_{rs},C_{ic},C_{is}: correction coefficients to the argument of periapsis [rad], orbit radius [m], and inclination [rad] for the perturbations caused by variations in the Earth's gravity field, solar radiation pressure, and attraction from the Sun and the Moon.

The algorithm to convert ephemerides of each i^{th} individual SV to the SV ECEF coordinates (see Fig. 1) based on [6] is as follows.

1) Assume as constants:
   - $c = 299792458$: speed of electromagnetic wave through a vacuum [m/s],
   - $a_E = 6378137.0$: WGS84 Earth's equatorial radius or semi-major axis [m],
   - $b_E = 6356752.3142$: WGS84 Earth's polar radius or semi-minor axis [m],
   - $\mu = 3.986005\text{E}14$: WGS84 Earth's standard gravitational parameter [m^3/s^2],

- $F = \frac{-2\sqrt{\mu}}{c^2}$: relativistic constant in the term of SV clock offset [s/$\sqrt{\text{m}}$],
- ω_E = 7.2921151467E-5: WGS84 value of the Earth's rotation rate [rad/s].

2) Assume as variables input by the simulator's operator or by the simulator model:
- σ_p: 1-sigma propagation error (typical single-frequency error budget $\sigma_p \approx$7m [17]–[21]) [m],
- Δt_p: signal propagation time which equals 20.0E6/c for all visible satellites at the cold start of simulated GPS receiver [s],
- φ_t: true latitude of GPS antenna aboard ship from the mathematical model of ship in the simulator [rad],
- λ_t: true longitude of GPS antenna aboard ship from the mathematical model of ship in the simulator [rad],
- h_t: true height above WGS84 ellipsoid of GPS antenna aboard ship from the mathematical model of ship in the simulator [m],
- α_{mi}: i^{th} SV elevation mask [rad],
- t_l: local (ship) time of position-fixing.

3) Extract the required parameters from the RINEX navigation file for the current ship local time.

Find the time of ephemeris (t_{oe}) corresponding to t_l in the navigation file. Calculate t_k (time elapsed since t_{oe}) according to (1). t_k must account for time zone including daylight saving (t_z), leap seconds (l_s), and time delay of signal propagation (Δt_p). All components of t_k must be converted to seconds and t_l must be referenced to the start time of GPS clock (i.e.: 00h:00min:00s, 06.01.1980) and further offset to SV time:

$$t_k = t_l + t_z + l_s - \Delta t_p - (t_{oe} + 604800G_W) - (a_0 + a_1(t)_l - t_{oc}) + a_2(t_l - t_{oc})^2 + \Delta_{rel} \quad (1)$$

where Δ_{rel} is a small relativistic correction caused by the orbital eccentricity:

$$\Delta_{rel} = F\sqrt{a}e\sin E_k \quad (2)$$

calculated after input from (3).

If $t_k > 302400$s subtract 604800s from t_k.

If $t_k < -302400$s add 604800s to t_k.

4) Compute initial orbital parameters for SV at time t_k as follows. Mean anomaly [rad]:

$$M_k = M_0 + (\sqrt{\mu}\Big/a^3 + \Delta_n)t_k \quad (3)$$

Eccentric anomaly from Kepler's equation (solved numerically by iteration with the initial value of $E_k = M_k$) [rad]:

$$E_k = M_k + e\sin E_k \quad (4)$$

True anomaly [rad]:

$$v_k = \arctan\left(\frac{\sqrt{1-e^2}\sin E_k}{\cos E_k - e}\right) \quad (5)$$

Argument of latitude (the angle between the ascending node and the SV) [rad]:

$$\Phi_k = v_k + \omega_0 \quad (6)$$

5) Adjust for orbital perturbations as presented below. Corrected argument of latitude [rad]:

$$u_k = \Phi_k + C_{\omega c}\cos 2\Phi_k + C_{\omega s}\sin 2\Phi_k \quad (7)$$

Corrected SV radial distance [m]:

$$r_k = a(1 - e\cos E_k) + C_{rc}\cos 2\Phi_k + C_{rs}\sin 2\Phi_k \quad (8)$$

Corrected inclination [rad]:

$$i_k = i_0 + i' t_k + C_{ic}\cos 2\Phi_k + C_{is}\sin 2\Phi_k \quad (9)$$

6) Compute the right ascension (corrected longitude of ascending node) accounting for Earth's rotation (ω_E) [rad]:

$$\Omega_k = \Omega_0 + (\dot{\Omega} - \omega_E)t_k - \omega_E t_{oe} \quad (10)$$

7) Compute SV Cartesian position in orbital plane [m]:

$$\begin{aligned} x'_k &= r_k\cos u_k \\ y'_k &= r_k\sin u_k \end{aligned} \quad (11)$$

8) Convert SV position from orbital frame to ECEF frame [m]:

$$\begin{aligned} x_{Si} &= x'_k\cos\Omega_k - y'_k\cos i_k\sin\Omega_k \\ y_{Si} &= x'_k\sin\Omega_k + y'_k\cos i_k\cos\Omega_k \\ z_{Si} &= y'_k\sin i_k \end{aligned} \quad (12)$$

In the steps from 3) to 8), the matrix notation and Hadamard operators (elementwise product or division operation on matrices or vectors) may be used instead of scalar notation to speed up the computation. The matrix notation replaces the calculation for each i^{th} SV in a loop.

B. FROM ECEF SATELLITE POSITIONS TO THE ANTENNA'S POSITION OF GPS RECEIVER

Using an omnidirectional antenna located at the coordinates X(to be determined), a GPS receiver receives the combined signal of all visible SVs. Due to the properties of the signal, the receiver can separate the individual SVs' terms of this combination and extract the relative propagated code phase, satellite ID, and data content using a replica of the transmitted PRN code. Given the data and relative code phase offsets, the receiver can identify the propagation time delay Δt_{pi} of each individual satellite signal and "ranges" can be calculated as

$$R_{pi} = c \cdot \Delta t_{pi} \quad (13)$$

Since a GPS receiver is not synchronized with the GPS system time and it generally uses less accurate quartz oscillator, the receiver has a significant clock offset dt_R to the exact system time. The SV clock also has some synchronization error dt_{Si}. And besides these errors, there are other factors affecting each i^{th} pseudorange measurement [19]: T_{ri} is the tropospheric delay, $\alpha_i STEC_i$ is a frequency dependent ionospheric delay (where α_i is the conversion factor between the integrated electron density along the ray path $STEC_i$, and the signal delay at L1 frequency), $\Delta\rho_{rel}$ is relativistic path

range factor, K_R is the receiver instrumental delay, K_{Si} is the SV instrumental delay,M_i represents the effect of multipath, and ε_i is the remaining noise. Some of these factors can be modeled; for example, the tropospheric and ionospheric delay (either by models like Klobuchar ionospheric model or by models adopted in SBAS systems as presented in [18] and [19]). However, the user clock error and residuals of other factors cannot be corrected through received information. So, the measured pseudorange (13) will equal to:

$$R_{pi} = \rho_i + c\,(dt_R - dt_{Si}) + T_{ri} + \alpha_i STEC_i + \Delta\rho_{rel} + K_R - K_{Si} + M_i + \varepsilon_i \quad (14)$$

where ρ_i is the geometric range between the satellite and receiver Antenna Phase Centers (APCs) at emission and reception time:

$$\rho_i = \|X - X_{Si}\|_2 = \sqrt{(x - x_{Si})^2 + (y - y_{Si})^2 + (z - z_{Si})^2} \quad (15)$$

$\|X\|_2$ – Euclidean norm of vector X=[x y z]^T. And the pseudorange (14) with applied corrections to predictable components of the measurement error will be:

$$p_i = R_{pi} + cdt_{Si} - T_{ri} - \alpha_i STEC_i - \Delta\rho_{rel} - K_R + K_S - M_i = \rho_i + cdt_R + \varepsilon_i \quad (16)$$

or:

$$p_i = \rho_i + \delta \quad (17)$$

Geometrically, (17) can be interpreted as a sphere with the center of X_{Si} and the radius of $p_i - \delta$. So, the problem is limited to a solution of the non-linear system of (17) for all visible satellites. The solution can be obtained by iterative numerical method after the conversion into form of algebraic linear equations and then the use of weighted least squares (WLS) estimation technique [1], [16], [19].

The following algorithm (supplementing the one described in section **II.*A***) of GPS code-based point position-fixing (single point positioning – SPP) has been implemented in the ship handling simulator.

1) Find the visible satellites at epoch t_l:

Using the transformation matrix R (18), convert i^{th} SVs' ECEF positions to topocentric coordinate system expressed in terms of elevation (α_{Si}), azimuth (A_{Si}), and range (ρ_i) at true position (φ_t, λ_t, h_t) read from the mathematical model of ship. Inputting false values of (φ_t, λ_t, h_t) instead of true values from the mathematical model of ship will lead to GPS spoofing simulation.

$$R = \begin{bmatrix} -\sin\varphi_t\cos\lambda_t & -\sin\varphi_t\sin\lambda_t & \cos\varphi_t \\ -\sin\lambda_t & \cos\lambda_t & 0 \\ \cos\varphi_t\cos\lambda & \cos\varphi_t\sin\lambda_t & \sin\varphi_t \end{bmatrix} \quad (18)$$

$$\begin{bmatrix} x_{Sti} \\ y_{Sti} \\ z_{Sti} \end{bmatrix} = R \begin{bmatrix} x_{Si} \\ y_{Si} \\ z_{Si} \end{bmatrix} \quad (19)$$

$$\rho_i = \sqrt{x_{Sti}^2 + y_{Sti}^2 + (z)_{Sti} - h_t{}^2} \quad (20)$$

$$A_{Si} = \arctan\frac{y_{Sti}}{x_{Sti}} \quad (21)$$

$$\alpha_{Si} = \frac{\pi}{2} - \arccos\frac{z_{Sti}}{d_i} \quad (22)$$

Select SVs that meet the condition of visibility over elevation mask α_{mi}:

$$\alpha_{Si} > \alpha_{mi} \quad (23)$$

Setting of α_{mi} can be also used for simulation of SVs obscured by an external infrastructure.

2) Adopt initial provisional values of x_0, y_0, z_0, δ_0 and relate them to unknown x, y, z,δ with the adjustment vector Δ:

$$\begin{cases} x = x_0 + \Delta_x \\ y = y_0 + \Delta_y \\ z = z_0 + \Delta_z \\ \delta = \delta_0 + \Delta_\delta \end{cases} \quad (24)$$

3) Add noise to the measured pseudoranges as a random variable distributed normally with mean $\mu = 0$ and variance σ_{pi}^2 (according to (17)):

$$p_i = \rho_i + N(0, \sigma_{pi}^2) \quad (25)$$

4) Build the system of linear algebraic equations (SLAE): Δ_x, Δ_y, Δ_z, Δ_δ are the unknown variables. Using Taylor-series expansion of (17) with respect to the assumed GPS position and the receiver's clock offset:

$$\begin{aligned} p_i &= f(x, y, z, \delta) = f(x_0, y_0, z_0, \delta_0) \\ &+ \frac{\partial f(x_0, y_0, z_0, \delta_0)}{\partial x_0}\Delta_x + \frac{\partial f(x_0, y_0, z_0, \delta_0)}{\partial y_0}\Delta_y \\ &+ \frac{\partial f(x_0, y_0, z_0, \delta_0)}{\partial z_0}\Delta_z + \frac{\partial f(x_0, y_0, z_0, \delta_0)}{\partial \delta_0}\Delta_\delta \\ &+ \frac{1}{2!}\frac{\partial^2 f(x_0, y_0, z_0, \delta_0)}{\partial x_0^2}\Delta_x^2 + \ldots \end{aligned} \quad (26)$$

Truncate (26) to the linear terms obtained as the first partial derivatives:

$$\begin{aligned} a_{1i} &= \frac{\partial f\ (x_0, y_0, z_0, \delta_0)}{\partial x_0} \\ &= \frac{x_0 - x_{Si}}{\sqrt{(x_0 - x_{Si})^2 + (y_0 - y_{Si})^2 + (z_0 - z_{Si})^2}} \\ a_{2i} &= \frac{\partial f\ (x_0, y_0, z_0, \delta_0)}{\partial y_0} \\ &= \frac{y_0 - y_{Si}}{\sqrt{(x_0 - x_{Si})^2 + (y_0 - y_{Si})^2 + (z_0 - z_{Si})^2}} \\ a_{3i} &= \frac{\partial f\ (x_0, y_0, z_0, \delta_0)}{\partial z_0} \\ 8 &= \frac{z_0 - z_{Si}}{\sqrt{(x_0 - x_{Si})^2 + (y_0 - y_{Si})^2 + (z_0 - z_{Si})^2}} \\ a_{4i} &= \frac{\partial f(x_0, y_0, z_0, \delta_0)}{\partial \delta_0} = 1 \end{aligned} \quad (27)$$

Combine (26) and (27):

$$p_i = \sqrt{(x_0 - x_{Si})^2 + (y_0 - y_{Si})^2 + (z_0 - z_{Si})^2} + \delta_0 + a_{1i}\Delta_x + a_{2i}\Delta_y + a_{3i}\Delta_z + a_{4i}\Delta_\delta \quad (28)$$

Introduce:

$$b_i = p_i + \sqrt{(x_0 - x_{Si})^2 + (y_0 - y_{Si})^2 + (z_0 - z_{Si})^2} - \delta_0 \quad (29)$$

And get the SLAE:

$$a_{1i}\Delta_x + a_{2i}\Delta_y + a_{3i}\Delta_z + a_{4i}\Delta_\delta = b_i \quad (30)$$

Or in the matrix form: $A\Delta = B$ where A is the observation or geometry matrix:

$$A = \begin{bmatrix} a_{11} & a_{12} & a_{13} & a_{14} \\ a_{21} & a_{22} & a_{23} & a_{24} \\ \cdots & \cdots & \cdots & \cdots \\ a_{n1} & a_{n2} & a_{n3} & a_{n4} \end{bmatrix} \quad (31)$$

Δ and B equal:

$$\Delta = \begin{bmatrix} \Delta_x \\ \Delta_y \\ \Delta_z \\ \Delta_\delta \end{bmatrix}, \quad \mathrm{B} = \begin{bmatrix} b_1 \\ b_2 \\ \cdots \\ b_n \end{bmatrix} \quad (32)$$

5) Seek the solution of vector Δ:

In general (30) is an overdetermined system. Its equations contain GPS-related noise. Taking into account the noise vector η (30) becomes:

$$A\Delta = B - \eta \quad (33)$$

The WLS solution of (33) is optimal as a maximum likelihood estimation of the regression problem if the observation noise is normally distributed (assumed to be zero-mean white-noise):

$$\Delta = (A^T WA)^{-1} A^T WB \quad (34)$$

where W is the diagonal weight matrix of (w_1, w_2, w_3,..., w_n) which is equal to inverse of a priori covariance matrix of the observations.

The values in this matrix are interpreted as weights of individual equations. For the ship handling simulation without GPS integrity monitoring these weights can be assumed to change in respect to elevation angle α_i[deg] according to example empirical exponential expression as the one elaborated in [24]:

$$w_i = \frac{\sigma_{pi}^2}{(5.504 + 35.26\exp(-\frac{\alpha_i}{10.14}))^2} \quad (35)$$

where σ_{pi}^2 corresponds to user equivalent range error. The basic idea behind the elevation-dependent weighting concept is that observations at lower elevation angles suffer more strongly from atmospheric and multipath effects, hence are more noisy than those at higher elevation angles. The elevation-dependent variance models assume a strong correlation between the satellite elevation angle and GPS signal quality. They become inefficient for observations which are strongly affected by multipath effects, signal diffraction and receiver characteristics. For measurements collected under non-ideal observational conditions, direct signal quality measures such as signal-to-noise ratio (SNR) based variance models can be more appropriate to assess the quality of GPS observations. The weight matrix W can also be built under assumption of uncorrelated measurements characterized by the inverse variances of the estimated error components if SBAS data are used [18]– [27]:

$$W = \begin{bmatrix} \frac{1}{\sigma_1^2} & 0 & \cdots & 0 \\ 0 & \frac{1}{\sigma_2^2} & \cdots & 0 \\ \vdots & \vdots & \ddots & \vdots \\ 0 & 0 & \cdots & \frac{1}{\sigma_n^2} \end{bmatrix} \quad (36)$$

$$\sigma_i^2 = \sigma_{i,flt}^2 + \sigma_{i,UIRE}^2 + \sigma_{i,tropo}^2 + \sigma_{i,mr}^2 \quad (37)$$

where, in (37):

$\sigma_{i,flt}^2$ is the estimated variance for the residual error associated to user differential range error $\sigma_{i,\mathrm{UDRE}}$, which can be calculated per analogy to the model adopted in [18] from SBAS data [m^2],

$\sigma_{i,UIRE}^2$ is the estimated variance for the slant range ionospheric error associated to grid ionospheric vertical error $\sigma_{i,\mathrm{GIVE}}$, which can be calculated per analogy to the model of [18] from SBAS data [m^2],

$\sigma_{i,tropo}^2$ is the estimated variance for the residual tropospheric error, which can be calculated per analogy to the model of [18] from SBAS data [m^2],

$\sigma_{i,mr}^2$ is the estimated variance of shipborne receiver error depending on the receiver's properties, and site-specific GNSS signal propagation effects like multipath, which must be locally evaluated (this alone variance cannot be derived from the SBAS message) [m^2].

Ideally, σ_i should strictly encompass σ_{pi}. In practice some integrity risk of the resultant protection level remains. The value of this risk can be modified by setting of protection level's coverage factor [28].

6) Repeat the algorithm from step 2) until max $|\Delta| \leq 0.0001$m (numerical approximation of solution to less than submillimetre is insignificant in the process of code measurements for transport applications) substituting the previous provisional values of x_0, y_0, z_0, δ_0 with: $x_0 + \Delta_x$, $y_0 + \Delta_y$, $z_0 + \Delta_z$, $\delta_0 + \Delta_\delta$.

The unknowns x, y, z,δ in (24) will be found after several iterations, and Δt_{pi} in (1) will be updated.

7) Convert the ECEF x, y, z to geodetic (ellipsoidal) coordinates φ, λ, h (the commonly used conversion formulas are discussed in [16], [20] or [25]).

The remaining issue is calculation of the ship's instant velocity as speed and course over ground (SOG and COG).

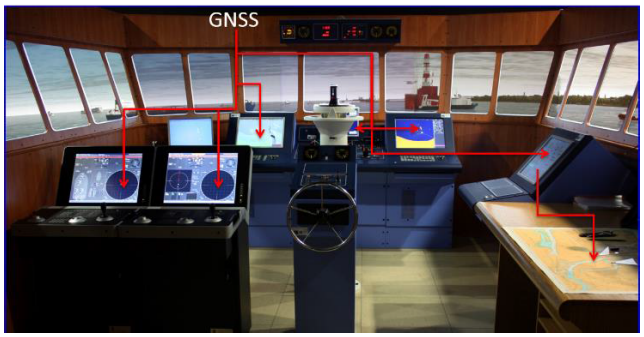

FIGURE 2. FMBS of kongsberg polaris type.

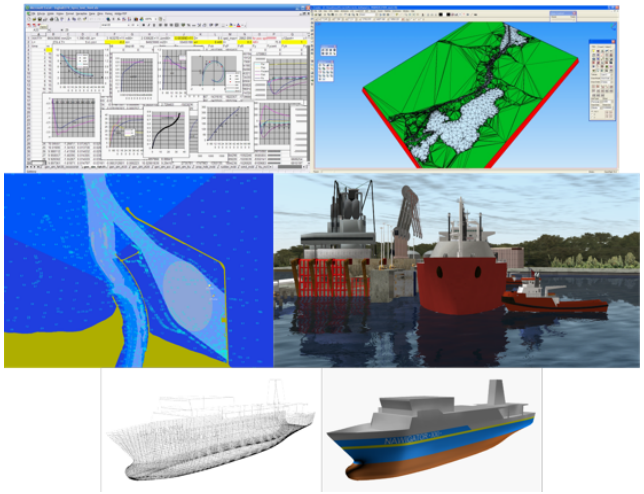

FIGURE 3. The construction of the simulation environment in FMBS.

Basic observables formed in GPS receivers are pseudoranges (16), representing apparent transit times of signals between GPS satellites and the receiver, scaled in the units of distance. The simplest methods of velocity calculation are algorithms processing only pseudoranges. The approximate derivatives of positions coordinates φ, λ, h estimated in successive time epochs can be used for this purpose. But some contemporary shipborne GPS receivers also form delta-ranges, based on Doppler frequency shift measurements. The delta-ranges are scaled in units of velocity and represent apparent relative velocities of the user with respect to SVs. The observables of pseudoranges and delta-ranges, along with the positions and velocities of SVs, calculated on the basis of data extracted from GPS navigation messages as in section **II.*A***, can be used to solve for the user's position, velocity and time (PVT) as well [16].

III. IMPLEMENTATION IN SHIP HANDLING SIMULATOR

A physical full-mission ship bridge simulators (FMBS) as presented in Fig. 2 contain high-fidelity hydrodynamic and visual models of vessels and navigation areas (Fig. 3).

They are utilized for sophisticated training and research activities in the environment that is operationally very close to reality. But GNSS models commercially-implemented into

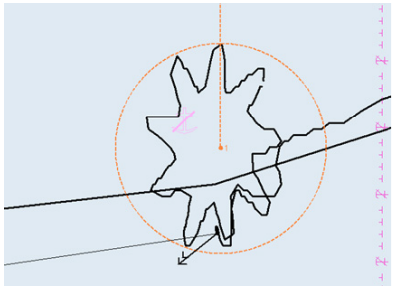

FIGURE 4. Example of GPS static position plot in FMBS.

FMBS are usually not suited for tasks where modeling of PNT data accuracy and integrity is essential [23]–[28].

Fig. 4 shows the ECDIS screen of one of the commercially available FMBS with 30min. record of stationary GPS position colored black. It is evident that the set GPS position error (7m marked by orange range marker) is applied as a maximum one with quite unrealistic cyclic changes of residuals.

Instead of these far too simplistic models, the algorithms presented in sections **II.*A*** and **II.*B*** should be run consecutively during ship motion simulation to get a position update rate of at least one second as recommended by IMO [12], [14], [15]. It is worth noting that the observation and measurement noise can be implemented in both algorithms. Equation (25) contains the component reflecting total propagation noise of each i^{th} SV, covering ionospheric, tropospheric, and equipment uncertainties. On the other hand, observation noises of SVs positions can be similarly included in (12). Also, the problem of ship's velocity calculation can be solved either by 1) the algorithm utilizing generated delta-ranges [16] or by 2) Kalman filtering which can be roughly summarized as the WLS SPP solution of (33) augmented with a prediction of the estimates as additional equations [7]–[29]. The determination of the state transition matrix and process noise matrix in Kalman filter can be based on physical kinematic model. If a vessel is moving at some velocity, the position coordinates' changes will be modeled by the laws of motion which make the position estimate dependent on velocity and acceleration with uncertainty growing with time. Finally the process will lead to estimation of user instant speed and course over ground but with cost of extra time correlated errors dependent on Kalman gain and ship's dynamics.

The GPS SPP model presented in section **II**. has been implemented in Matlab$^{\text{TM}}$ and C# programming environment as an alternative to GNSS component built in a commercial FMBS. Several simulation scenarios with constant and variable 1-sigma GPS propagation error (σ_{pi}) were performed. Figures 5, 6, 7 present results of the scenario where the shipborne GPS antenna is stationary, and the standard deviation of all SVs measurements is constant: $\sigma_{pi} = 7.1$m.

The example of calculated GPS position-fix is shown in Fig. 5 as a yellow mark on the surface of the Earth with momentary SVs positions marked by red diamonds.

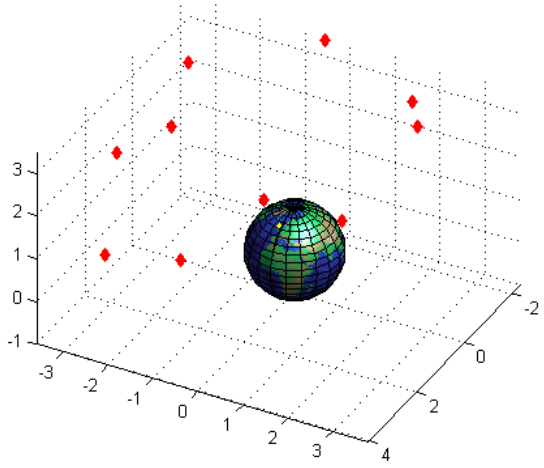

FIGURE 5. The ECEF plot of the simulated GPS SVs in units of earth radius ratio.

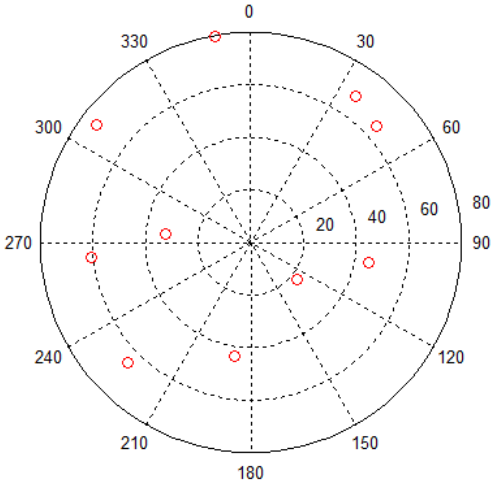

FIGURE 6. The polar plot of the simulated GPS SVs azimuth and zenith distances [°].

The corresponding polar plot of SVs positions marked by red circles (converted to topocentric azimuth and zenith distances from GPS position-fix) is shown in Fig. 6.

The distribution of 30 GPS two-dimensional positions (blue dots) recorded every minute is shown in the Fig. 7. This position plot, constructed after the conversion of ellipsoidal coordinates to local north-east-up (NEU) metric coordinates, reflects the SV pseudorange error propagation to the final user position error and the evident impact of SVs geometry on the position distribution (N-S variation for the latitude and epoch selected is significantly larger than E-W). The 2DRMS (twice distance root mean square) positioning error is approximately 10m.

IV. MODEL VERIFICATION

Verification of the developed model was carried out using the Ashtech ^{TM} MB100 receiver module shown in Fig. 8.

The reception was set to GPS system only, the Kalman filtering was disabled, and the antenna position was fixed

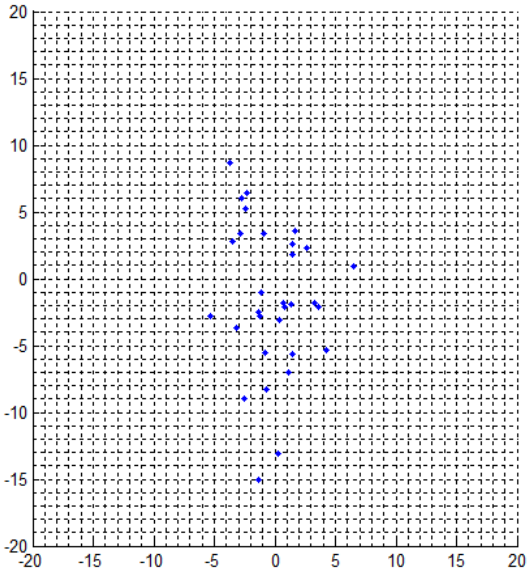

FIGURE 7. The simulated GPS position plot in the local metric system.

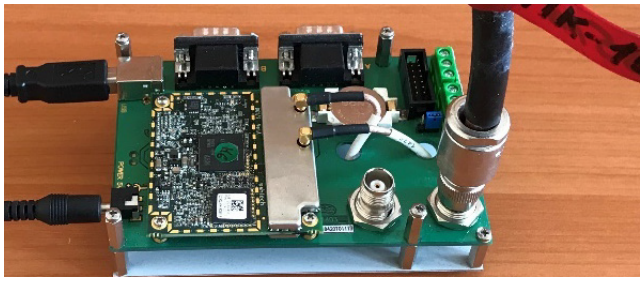

FIGURE 8. Ashtech ^{TM} OEM GNSS receiver module used in the research.

stationary on the upper-top deck of the test ship moored in harbor during data recording.

Fig. 9 and 10 present examples of position records from one day - 24h (at the plot in Fig. 9), and from 1h (at the plot in Fig. 10) in relation to the precise antenna position at (0,0) estimated by Network Real Time Kinematic technique with 2DRMS less than 3cm. The analyzed data were collected on 08.07.2018 between 00:00:00 – 23:59:59 UTC with 1s update rate. The data from 19:00:00-19:59:59 were selected for 1h position record respectively. They were converted from WGS84 geographic coordinates to local NEU metric coordinates.

One can notice a large variation and bias of the determined position-fix during a full day (24h), yet lower variation within much shorter period (one hour). Analysis of the recorded data led to conclusion that adding normally distributed noise to the measured pseudoranges as in (25) will not lead to realistic GNSS measurement model. (25) should be modified in order to reflect a significant dependency of propagation error on SV azimuth and elevation.

Taking this into account, the standard deviations of distributions of distances to the reference position within full hours σ_h and full minutes σ_m of one-month recording were determined. Additionally, to estimate the dynamics of position

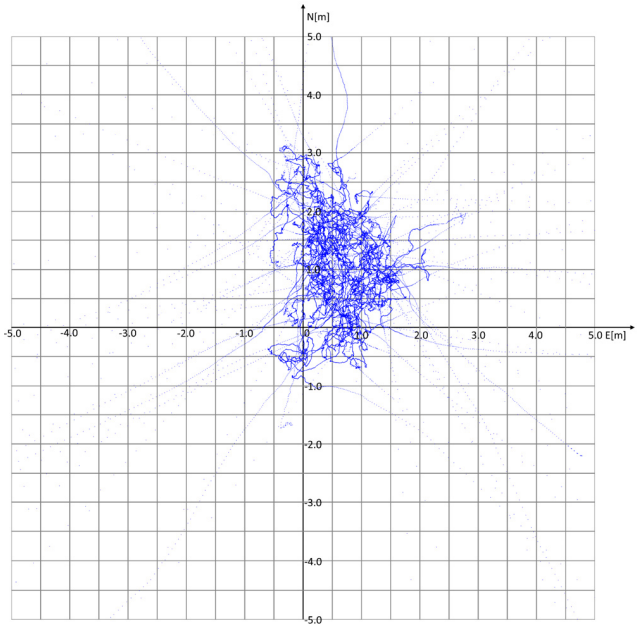

FIGURE 9. The example of 24h position records from a physical receiver.

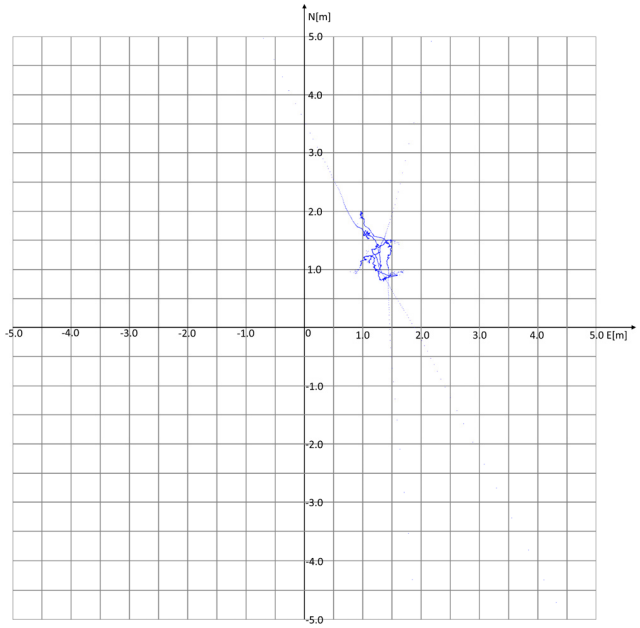

FIGURE 10. The example of 1h position records from a physical receiver.

change, the n_{hm} parameter (defined as the ratio of the mean σ_h to mean σ_m) was calculated.

$$n_{hm} = \frac{\bar{\sigma_h}}{\bar{\sigma_m}} \tag{38}$$

In order to simulate a slow-changing and azimuth-dependent propagation error (ionosphere TEC varies with the amount of sunshine) six sets of amplitude A_{azj} and phase φ_{azj} values for azimuths quantified to 0°, 60°, 120°, 180°, 240°, 300° were randomly selected.

$$A_{azj} = \left| N(0, \sigma_p^2) \right| \tag{39}$$

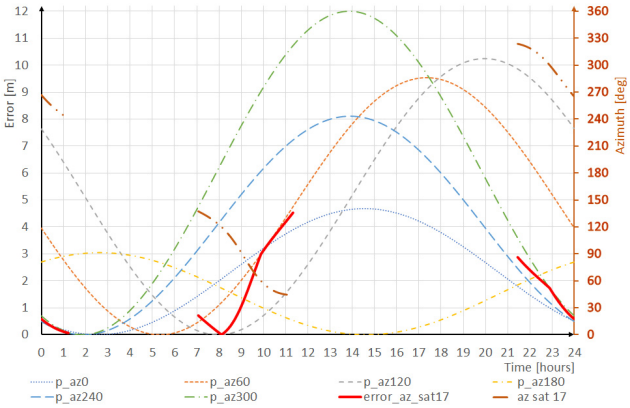

FIGURE 11. Example values of propagation error and azimuth for SV 17.

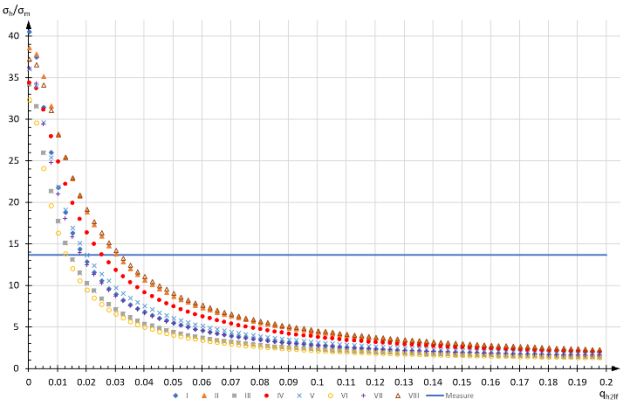

FIGURE 12. Relation between n_{hm} ratio and q_{h2lf} coefficient.

$$\varphi_{azj} = U\langle 0, 2\pi \rangle \tag{40}$$

The period of function U in (40) was set to 24h and the following variable and constant were assigned:
- t – the number of seconds from midnight,
- t_{day} – the number of seconds within 24h (86400s).

So, azimuth-dependent variable of the pseudorange error was defined as:

$$p_{azj} = A_{azj}(1 + \sin(2\pi t/t_{day} + \varphi_{azj}))/\sqrt{2} \tag{41}$$

And p_{azi}, corresponding to the specific azimuth of i^{th} satellite, was set by linear interpolation between errors determined for the nearest p_{azj} azimuths. Finally (25) was modified to:

$$p_i = d_i + q_{h2lf} |N\left(0, \sigma_{pi}^2\right)| + (1 - q_{h2lf}) p_{azj} \tag{42}$$

after assignment of q_{h2lf} as a simulation coefficient corresponding to n_{hm} in (38), Fig. 11 shows example values of azimuth component of the propagation error for the satellite PRN 17 per one day. Respectively the symbols in Fig. 11 mean: *p_az0* is $p_{az0°}$, *p_az60* is $p_{az60°}$, and so on, *az sat 17* is SV azimuth, and *error_az_sat17* is p_{17} calculated according to (42). Based on this figure it is possible to check how the error estimation is simulated. At 9:00AM satellite PRN 17 had azimuth of 91.6°, $p_{az60°} = 2.02$m,

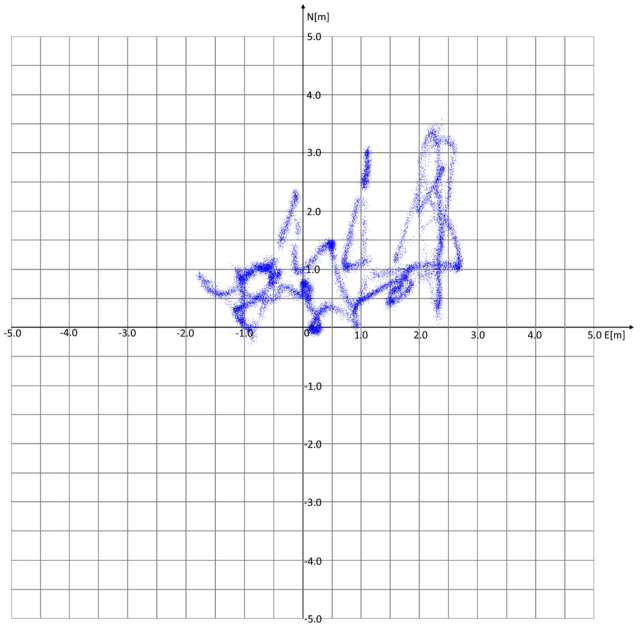

FIGURE 13. Simulated GPS position records from 24h.

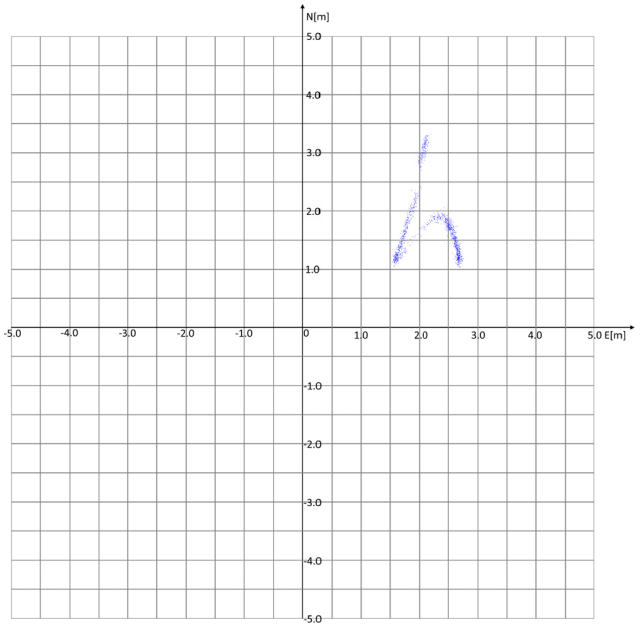

FIGURE 14. Simulated GPS position records from one hour.

$p_{az120^\circ} = 0.19$m, so:

$$p_{az91.6^\circ} = \frac{[2.02 \cdot (120 - 91.6) + 0.19 \cdot (91.660)]}{60} \approx 1.056 \text{ m} \quad (43)$$

Fig. 12 depicts σ_h to σ_m ratio depending on the q_{h2lf} parameter for eight random sets of A_{azj} amplitude and a φ_{azj} phase. The blue line is the reference value of n_{hm} (39) obtained from real measurements.

The adopted values of the parameters for the test-bed scenario were $\sigma_p = 7.1$m, and $q_{h2lf} = 0.0215$ which in Fig. 12 is the average value of the curves' intersection with the reference value. The amplitude values A_{azj} and phase values φ_{azj} were computed once during the simulation period. Fig. 13 and 14 present examples of simulated stationary position records (in blue) corresponding (time and location synchronized) to the actual position records in Fig. 9 and 10 after implementation of the elaborated GPS measurements model in FMBS.

It can be noticed that the bias and variation of simulated position records are similar to the ones shown in Fig. 9 and 10. Although, quite significant differences remain in general ''random walk'' distributions. The further research on several different makes/types of shipborne receivers and individual GNSS error components should lead to a better solution of this issue.

V. CONCLUSIONS

The paper elaborates on the model of GNSS positioning and GNSS error propagation into ship's final position coordinates in maritime simulators. Such a model becomes a key factor that enables a ship handling simulator to be utilized in the sophisticated training of navigators and in manoeuvring safety analyses, especially at the time of restricted visibility or jamming / spoofing of GNSS. This is one of the conditions for the compatibility of simulated navigation system with reality. The stochastic model of GPS code pseudorange observations has been embedded in a physical and virtual reality ship simulator for this purpose. The operator of ship handling simulator has been given access to modify 1-sigma estimations of propagation errors (consisting of the SV azimuth and elevation dependent variables of the pseudorange error) and ephemeris data (RINEX navigation data file) that correspond to simulation time. The further step of the research and constructed models' validation will be in-depth comparative analysis of scenarios designed in real and virtual environment respectively with several different makes of shipborne receivers and parameters of GNSS measurements' error model.

REFERENCES

[1] J. B.-Y. Tsui, *Fundamentals of Global Positioning System Receivers: A Software Approach*, 2nd ed. Hoboken, NJ, USA: Wiley, 2005. doi: 10.1002/0471712582.

[2] J. Bhatti and T. Humphreys, ''Hostile control of ships via false GPS signals: Demonstration and detection,'' *Navigat., J. Inst. Navigat.*, vol. 64, no. 1, pp. 51–66, 2017.

[3] A. Brown, J. Redd, and M.-A. Hutton, ''Simulating GPS signals. It doesn't have to be expensive,'' *GPS World May 2012*, vol. 23, no. 5, pp. 44–50, 2012.

[4] *Maritime Simulator Systems*, Standard DNVGL-ST-0033, DNV GL AS, Mar. 2017.

[5] L. A. Dobryakova, L. S. Lemieszewski, and E. F. Ochin, ''GNSS spoofing detection using static or rotating single-antenna of a static or moving victim,'' *IEEE Access*, vol. 6, pp. 79074–79081, 2018. doi: 10.1109/ACCESS.2018.2879718.

[6] G. Directorate. (Apr. 25, 2018). *Systems Engineering & Integration: Interface Specification IS-GPS-200*. Accessed: Oct. 16, 2018.[Online]. Available: https://www.gps.gov/technical/icwg/

[7] M. S. Grewal and A. P. Andrews, *Kalman Filtering: Theory and Practice With MATLAB*. 4th ed. Hoboken, NJ, USA: Wiley, 2015. doi: 10.1002/9781118984987.

[8] C. Hargreaves and P. Williams, ''Maritime integrity concept,'' in *Proc. Eur. Navigat. Conf. ENC*, J. Johansson and G. Elgered, Eds. Gothenburg, Sweden: Chalmers Univ. Technology, 2018, pp. 120–127, Accessed 19 Oct. 2018. [Online]. Available: https://enc2018.eu/programme/

[9] T. E. Humphreys, B. A. Ledvina, M. L. Psiaki, B. W. O'Hanlon, and P. M. Kitner, "Assessing the spoofing threat," *GPS World January 2009*, vol. 20, no. 1, pp. 28–38, 2009.

[10] K. Hünerbein and W. Lange, "Testing telemetry systems, which use GNSS satellite navigation systems achieving reliable and accurate results with RF simulation of GNSS signals," in *Proc. 36th Eur. Telemetry Test Conf.*, 2016, pp. 40–46 Nürnberg, Germany. doi: 10.5162/etc2016/1.5.

[11] (2015). *RTCM-SC104: RINEX The Receiver Independent Exchange Format, Version 3.03*. Accessed Oct. 16, 2018. [Online]. Available: ftp://igs.org/pub/data/format/rinex303.pdf

[12] (2017). Circular MSC.1/Circ.1575: Guidelines for Shipborne Position, Navigation and Timing Data Processing, International Maritime Organization, London, U.K., Accessed: Oct. 19, 2018. [Online]. Available: http://www.imo.org/en/OurWork/Circulars/Pages/Home.aspx

[13] (2015). Resolution MSC.401(95), Performance Standards for Multi-System Shipborne Radionavigation Receivers, International Maritime Organization, London, U.K., amended by Resolution MSC.432(98), International Maritime Organization. Accessed: Oct. 19, 2018.[Online]. Available: http://www.imo.org/en/KnowledgeCentre/IndexofIMOResolutions/Maritime-Safety-Committee-(MSC)/Documents/MSC.401(95).pdf and http://www.imo.org/en/KnowledgeCentre/IndexofIMOResolutions/Maritime-Safety-Committee-%28MSC%29/Documents/MSC.432

[14] (2011). Resolution A.1046(27). Worldwide Radionavigation System, International Maritime Organization, London, U.K., Accessed: Oct. 19, 2018. [Online]. Available: http://www.imo.org/en/KnowledgeCentre/Indexof IMOResolutions/Documents/A%20-%20Assembly/1046(27).pdf

[15] (2001). Resolution A.915(22), Revised Maritime Policy and Requirements for a Future Global Navigation Satellite System (GNSS), International Maritime Organization, London, U.K., Accessed: Oct. 19, 2018. [Online]. Available: http://www.imo.org/blast/blastData.asp?doc_id=10904&filename=A%20915%2822%29.pdf

[16] E. Kaplan and C. Hegarty, *Understanding GPS: Principles and Applications*, 2nd ed. Norwood, MA, USA: Artech House, 2006.

[17] M. Kim and J. Kim, "A long-term analysis of the GPS broadcast orbit and clock error variations," in *Proc. Asia–Pacific Int. Symp. Aerosp. Technol. (APISAT)*, 2015, pp. 654–658.doi: 10.1016/j.proeng.2014.12.585.

[18] *Minimum Operational Performance Standards for Global Positioning System/Satellite-Based Augmentation System Airborne Equipment*, Standard DO-229E, RTCA, 2016.

[19] S. J. Sanz, J. M. Juan Zornoza, and M. Hernández-Pajares, *GNSS Data Processing Volume I: Fundamentals and Algorithms*, document ESTEC TM-23/l, ESA Communications, Noordwijk, The Netherlands, 2013.

[20] C. Shu and F. Li, "An iterative algorithm to compute geodetic coordinates," *Comput. Geosci.*, vol. 36, no. 9, pp. 1145–1149, Sep. 2010. doi: 10.1016/j.cageo.2010.02.004.

[21] (2008). *GPS Standard Positioning Service Performance Standards*. Accessed: Oct. 19, 2018. [Online]. Available: https://www.gps.gov/technical/ps/2008-SPS-performance-standard.pdf

[22] S. Thombre, M. Zahidul, H. Bhuiyan, P. Eliardsson, B. Gabrielsson, M. Pattinson, M. Dumville, D. Fryganiotis, S. Hill, V. Manikundalam, M. Pölöskey, S. Lee, L. Ruotsalainen, S. Söderholm, and H. Kuusniemi, "GNSS threat monitoring and reporting: Past, present, and a proposed future," *J. Navigat.*, vol. 71, no. 3, pp. 513–529, 2018. doi: 10.1017/S0373463317000911.

[23] J. Wang and P. B. Ober, "On the availability of fault detection and exclusion in GNSS receiver autonomous integrity monitoring," *J. Navigat.*, vol. 62, no. 2, pp. 251–261, Apr. 2009. doi: 10.1017/S0373463308005158.

[24] D. H. Won, J. Ahn, S.-W. Lee, J. Lee, S. Sung, H.-W. Park, J.-P. Park, and Y. J. Lee, "Weighted DOP with consideration on elevation-dependent range errors of gnss satellites," *IEEE Trans. Instrum. Meas.*, vol. 61, no. 12, pp. 3241–3250, Dec. 2012. doi: 10.1109/TIM.2012.2205512.

[25] G. Xu, *Orbits*. Berlin, Germany: Springer-Verlag, 2008. doi: 10.1007/978-3-540-78522-4.

[26] P. Zalewski, "Real-time GNSS spoofing detection in maritime code receivers," *Sci. J. Maritime Univ. Szczecin*, vol. 38, no. 110, pp. 118–124, 2014. [Online]. Available: http://repository.scientific-journals.eu/handle/123456789/608

[27] P. Zalewski, "Presentation of satellite based augmentation system integrity data in an electronic chart system display," *Sci. J. Maritime Univ. Szczecin*, vol. 45, no. 117, pp. 150–156, 2016. doi: 10.17402/099.

[28] P. Zalewski, L. Gucma, S. Gewies, K. Urbanska, S. Schlueter, and M. Porretta, "Concept of EGNOS implementation in the maritime domain," in *Proc. ESA NAVITEC*, 2016, sec. A3, pp. 1–14. Accessed: Oct. 19, 2018. [Online]. Available: http://www.proceedings.com/33604.html

[29] P. Zarchan and H. Musoff, *Fundamentals of Kalman Filtering: A Practical Approach*, 4th ed. vol. 246, T. C. Lieuwen. Atlanta, Georgia: Georgia Institute Technology,, 2015.

PAWEŁ ZALEWSKI received the M.S. degree in navigation from the Maritime University of Szczecin (MUS), in 1994, and the Ph.D. degree in geodesy and cartography, in 2001. From 1995 to 2001, he was a Research Assistant with the Marine Traffic Engineering Centre, Institute of Marine Traffic Engineering, MUS, where he was an Assistant Professor, from 2001 to 2014. He received the Postdoctoral degree in transport from Radom Technical University, in 2014. From 2014 to 2016, he was the Managing Editor of the *European Journal of Navigation* issued by EUGIN. Since 2011, he has been in charge of dynamic positioning training, MUS, a Nautical Institute Member, since 2014, an Associate Professor with MUS, and since 2016, elected as the Dean of Navigation Faculty, MUS. He has four years of experience on board sea-going vessels at operational and management levels. He is currently a Lecturer in navigation systems and applied mathematics for navigation and marine transport engineering students of bachelor's and master's degrees. He has authored three books, coauthored four books and more than 90 articles. He holds two patented inventions. His research interests include navigation systems, safety of navigation, and marine traffic engineering. Since 2008, he has been a member of the Polish Navigation Forum and an Expert of Polish Delegation to NAV and NCSR subcommittees to IMO.

MATEUSZ BILEWSKI received the M.S. degree in electronics from the West Pomeranian University of Technology, in 2010. From 2010 to 2011, he was a Research Assistant with the Institute of Marine Traffic Engineering, Maritime University of Szczecin (MUS), where he has been a Research Assistant with the Marine Traffic Engineering Centre, since 2011. In 2017, he started the Ph.D. research on the subject of data fusion from navigation systems, such as 2D laser scanners and GNSS. He conducts classes in navigational equipment and programming of marine simulators. He has coauthored one book and more than 20 articles. His research interests include navigation systems, safety of navigation, and marine traffic engineering.